Measurement of Normalised Cross Sections for Jet Production in ep Collisions at HERA and Comparison to Next-to-next-to-leading Order QCD Predictions

H1 Collaboration

Abstract

A measurement of jet cross sections in neutral current deep-inelastic scattering normalised to the neutral current deep-inelastic scattering inclusive cross sections is presented and compared to next-to-leading order and novel next-to-next-to-leading order prediction in perturbative QCD.

1 Results and Discussions

Cross sections for jet production in neutral-current deep-inelastic ep scattering (NC DIS) are measured using data taken with the H1 experiment in the years 2006 and 2007 during the HERA-II running period, corresponding to an integrated luminosity of $184\,\mathrm{pb}^{-1}$. The kinematic range is defined by the exchanged photon virtuality of $5.5 < Q^2 < 80\,\mathrm{GeV}^2$ and inelasticity $0.2 < y < 0.6$. Jets are defined in the Breit frame using the inclusive k_T cluster algorithm [1] with a distance parameter of $R = 1$ and are required to exceed a minimum jet transverse momentum in the Breit frame, P_T^{jet}, of 4.5 GeV and to have a pseudorapidity in the laboratory frame in the range $-1.0 < \eta_{\mathrm{lab}}^{\mathrm{jet}} < 2.5$.

The presented normalised jet cross sections are defined as the ratio of the double-differential absolute jet cross sections to the inclusive NC DIS cross section in the respective Q^2 bin. The calculation of the statistical uncertainties in this ratio takes the statistical correlations between the numerator and the denominator into account, since these are measured on detector level and propagated linearly through the unfolding process. Jet cross sections normalised to the NC DIS cross sections benefit from a full cancellation of normalisation uncertainties and partial cancellation of other experimental uncertainties. Absolute jet cross sections, i.e. not normalised to the inclusive NC DIS cross sections, based on the same dataset, have already been presented in ref. [2].

Normalised dijet and trijet cross sections, where events with at least two or three jets are counted, are obtained as a function of Q^2 and the average transverse momentum of the two or three leading jets, $\langle P_T \rangle_2$ and $\langle P_T \rangle_3$, respectively, in the ranges $5 < \langle P_T \rangle_2 < 50\,\mathrm{GeV}$ and $5.5 < \langle P_T \rangle_3 < 40\,\mathrm{GeV}$. Normalised inclusive jet cross sections, where every individual jet is counted, are obtained as a function of Q^2 and P_T^{jet} in the range $4.5 < P_T^{\mathrm{jet}} < 50\,\mathrm{GeV}$.

In addition, normalised inclusive jet cross sections are further presented in the range $5 < P_T^{\mathrm{jet}} < 7\,\mathrm{GeV}$ for higher values of Q^2 in the range $150 < Q^2 < 15\,000\,\mathrm{GeV}$. These new high-$Q^2$ measurements extend the kinematic range of an earlier analysis of H1 HERA-II data [3] and related details on these high-Q^2 inclusive jet measurements are found in ref. [3]. The studies performed within the scope of this analysis improved the understanding of low-P_T^{jet} jets and also validated the estimation of the uncertainties. Now these additional data points are given.

Jet cross sections are obtained using regularised unfolding procedure as implemented in the TUnfold [4] package, where cross sections for the NC DIS, inclusive jet, dijet and trijet production are unfolded simultaneously and the statistical correlations are taken into account in this procedure. The kinematic migrations are determined with the two Monte Carlo event generators Djangoh [5] and Rapgap [6]. The data are corrected for photoproduction background contributions ($Q^2 < 2\,\mathrm{GeV}^2$) using the Pythia event generator [7], and the background is found to be almost negligible for jet cross sections. The data are corrected for higher-order QED radiative effects.

The cross sections are obtained double-differentially as a function of Q^2 and P_T, where P_T denotes the transverse momenta of the individual jets for inclusive jets or the average transverse momenta of the two or three leading jets with the highest P_T^{jet} in case of dijet and trijet cross sections. The kinematic range of the cross sections is summarised in table 1.

The data are compared in figs. 1 to 6 to theoretical predictions in perturbative QCD (pQCD). The predictions are summarised in table 2 and described briefly in the following:

	Phase space low-Q^2	**Phase space high-Q^2**
NC DIS phase space	$5.5 < Q^2 < 80\,\text{GeV}^2$	$150 < Q^2 < 15{,}000\,\text{GeV}^2$
	$0.2 < y < 0.6$	$0.2 < y < 0.7$
Phase space common for all jets	$-1.0 < \eta_{\text{lab}}^{\text{jet}} < 2.5$	$-1.0 < \eta_{\text{lab}}^{\text{jet}} < 2.5$
	$P_{\text{T}}^{\text{jet}} > 4\,\text{GeV}$	
Inclusive jet	$4.5 < P_{\text{T}}^{\text{jet}} < 50\,\text{GeV}$	$5 < P_{\text{T}}^{\text{jet}} < 7\,\text{GeV}$
Dijet	$N_{\text{jet}} \geq 2$	
	$5 < \langle P_{\text{T}} \rangle_2 < 50\,\text{GeV}$	
Trijet	$N_{\text{jet}} \geq 3$	
	$5.5 < \langle P_{\text{T}} \rangle_3 < 40\,\text{GeV}$	

Table 1: Summary of the phase space of the presented normalised jet cross sections. Normalised jet cross sections at high values of Q^2 are further presented in ref. [3].

Predictions	**NLO**	**aNNLO**	**NNLO**
Jet cross sections			
Program	nlojet++	JetViP	NNLOJET
pQCD order	NLO [8]	approximate NNLO [12]	NNLO [15]
Calculation detail	Dipole subtraction	NLO plus NNLO contributions from unified threshold resummation formalism	Antenna subtraction
NC DIS cross sections			
Program	QCDNUM	APFEL	APFEL
Heavy quark scheme	ZM-VFNS	FONLL-C	FONLL-C
Order	NLO	NNLO	NNLO
PDF	NNPDF3.0_NLO	NNPDF3.0_NNLO	NNPDF3.0_NNLO
$\alpha_{\text{s}}(M_{\text{Z}})$	0.118	0.118	0.118
Hadronisation corrections	Djangoh and Rapgap		
Available for			
Normalised inclusive jet	✓	✓	✓
Normalised dijet	✓		✓
Normalised trijet	✓		

Table 2: Summary of the theory predictions for the normalised jet cross sections. All predictions are corrected for hadronisation effects with multiplicative corrections factors obtained from Djangoh and Rapgap.

- Predictions in next-to-leading order (NLO) are obtained using the program nlojet++ [8] interfaced to the package fastNLO for jet cross sections. For the NC DIS cross sections in the denominator of the normalised jet cross sections the program QCDNUM [9], using zero-mass variable-flavor-number scheme (ZM-VFNS), in NLO is used. The PDF set NNPDF3.0_NLO_AS_0118 [10] and a value for the strong coupling constant $\alpha_s(M_Z) = 0.118$ are used.

- Predictions for inclusive jet cross sections are obtained from the program JetViP [11] in approximate next-to-next-to-leading order (aNNLO) [12] applying the unified threshold resummation formalism. The NC DIS cross sections are obtained from the NNPDF Collaboration and are done consistently as in the NNPDF30 PDF extraction, using the program APFEL [13] in NNLO and applying the FONLL-C heavy quark scheme [14]. It was validated that predictions using QCDNUM and APFEL are identical for the ZM-VFNS. The PDF set NNPDF3.0_NNLO_AS_0118 and a value for the strong coupling constant $\alpha_s(M_Z) = 0.118$ are used for the jet and the NC DIS cross sections. These novel predictions are compared for the first time to inclusive jet cross section at the low-Q^2 kinematic domain.

- Predictions in full next-to-next-to-leading order pQCD (NNLO) [15] are obtained from the program NNLOJET [15, 16] for inclusive jet and dijet production, where the infrared and collinear singularities are cancelled using the antenna subtraction method. The NC DIS predictions are identical to the ones used as for the aNNLO predictions. The PDF set NNPDF3.0_NNLO_AS_0118 and a value for the strong coupling constant $\alpha_s(M_Z) = 0.118$ are used for the jet and the NC DIS cross sections. This is the first presentation and comparison to data of inclusive jet cross sections in full NNLO.

- The inclusive NC DIS cross sections are very well described by the theoretical prediction in NLO within the experimental uncertainties, while in NNLO the predictions undershoot the data up to 7 % at lowest values of Q^2. Such low Q^2 data were however not included in the determination of the used PDFs.

- The predictions for normalised jet cross sections are corrected for hadronisation effects applying bin-wise multiplicative correction factors. These are defined as the ratio of cross sections at hadron level to the parton level, i.e. before hadronisation took place and are determined with the help of the two Monte Carlo event generators: Djangoh [5] and Rapgap [6]. The applied factors are defined as the average correction factors from the two models.

- The renormalisation and factorisation scale for the calculation of the jet cross sections in the numerator are set as a rule to $\mu_r^2 = \mu_f^2 = \frac{1}{2}(Q^2 + P_T^2)$, where P_T denotes P_T^{jet}, $\langle P_T \rangle_2$ or $\langle P_T \rangle_3$ for inclusive jet, dijet or trijet cross sections respectively[1]. The renormalisation and factorisation scales are chosen to be Q^2 for the NC DIS calculations.

- Uncertainties on the theory predictions in NLO and NNLO are obtained from scale variations, where the renormalisation and factorisation scales are varied independently in the

---

[1] For the normalised dijet cross sections, and inclusive jet cross sections for Q^2 values of $Q^2 > 150\,\text{GeV}$, the factorisation scale is chosen to be $\mu_f^2 = Q^2$ for NLO and NNLO, because the NNLO calculations were not yet performed for the choice of $\mu_f = \mu_r$ at the time of writing this report.

numerator by factors 0.5, 1 and 2. The uncertainties are defined as the maximum and the minimum result from the nine possible variations, excluding the two variations with the factor 0.5 for one scale and 2 for the other.

- The running of the fine-structure constant α_{em} is identically defined for the jet and the NC DIS calculations, using the implementation of EPRC [17] in xFitter [18], such that this term cancels in the ratio.

The sensitivity of the new normalised jet cross section data to the strong coupling constant at the Z-boson mass and to the running of $\alpha_{\text{s}}(\mu_r)$ is studied in a fit of NLO predictions to data and shown in fig. 8. The χ^2 definition is given in ref. [3] and uncertainties from the PDFs and on the hadronisation corrections are further considered in this definition. The data points for normalised inclusive jet, dijet and trijet production are grouped into six groups with comparable values of μ_r and the value of $\alpha_{\text{s}}(M_{\text{Z}})$ is obtained from minimising χ^2. The value of $\alpha_{\text{s}}(\mu_r)$ is calculated from $\alpha_{\text{s}}(M_{\text{Z}})$ by applying the solution for the evolution equation of $\alpha_{\text{s}}(\mu_r)$. The scale uncertainty is obtained by repeating the fits with the six different choices for scale factors of 0.5 and 2. The new data probe the running of the strong coupling constant in the range of approximately $5 < \mu_r < 35\,\text{GeV}$. The uncertainties on the NLO predictions dominate significantly over the experimental uncertainties.

To improve the sensitivity to the strong coupling, also data points from the high-Q^2 domain may be considered in the fit [3]. A fit to all these 196 H1 HERA-II low- and high-Q^2 normalised jet cross section data points, where experimental correlations are considered, yields an experimental precision on $\alpha_{\text{s}}(M_{\text{Z}})$ of about 4 permille. Relevant theoretical uncertainties, higher than the experimental uncertainties, are from the PDF uncertainties, the choice of the PDF set, the input value of $\alpha_{\text{s}}(M_{\text{Z}})$ to the PDF fit and the hadronisation corrections. However, an extraction of $\alpha_{\text{s}}(M_{\text{Z}})$ from NLO predictions is entirely limited through the scale uncertainties.

2 Summary

New measurements of jet cross sections in neutral current deep-inelastic scattering in the Breit frame normalised to the neutral current deep-inelastic inclusive scattering cross sections are presented. The data are compared to next-to-leading order prediction in perturbative QCD. Also new predictions in full next-to-next-to-leading order and approximate next-to-next-to-leading order are shown for the first time and compared to data.

It is found that the full next-to-next-to-leading order predictions improve the description of the normalised inclusive jet and normalised dijet data compared to next-to-leading order predictions. The approximate next-to-next-to-leading order predictions improve the description of the normalised inclusive jet data at higher values of the transverse momentum of the jets. The sensitivity of the data to the extraction of the strong coupling constant and to the running of the strong coupling is studied in a fit to next-to-leading order predictions. The experimental precision on an extraction of $\alpha_{\text{s}}(M_{\text{Z}})$ from the H1 HERA-II normalised jet data in the range $5.5 < Q^2 < 15\,000\,\text{GeV}$ is about 0.4 %.

References

[1] S. Ellis and D. Soper, *Phys. Rev.* **D48** (1993) 3160, [hep-ph/9305266].

[2] H1 Collaboration, H1prelim-16-61, available at:
    `https://www-h1.desy.de/publications/H1preliminary.short_list.html`

[3] H1 Collaboration, V. Andreev *et al.*, *Eur. Phys. J.* C **75** (2015) 2, [arXiv:1406.4709].

[4] S. Schmitt, *JINST* 7 (2012) T10003, [arXiv:1205.6201].

[5] K. Charchula, G. A. Schuler, and H. Spiesberger, *Comput. Phys. Commun.* **81** (1994) 381, DJANGOH V1.4.

[6] H. Jung, *Comp. Phys. Commun.* **86** (1995) 147, RAPGAP V3.1.

[7] T. Sjöstrand *et al.*, *Comput. Phys. Commun.* 135 (2001) 238, [hep-ph/0010017].

[8] Z. Nagy and Z. Trocsanyi, *Phys. Rev. Lett.* 87 (2001) 082001, [hep-ph/0104315].

[9] M. Botje, *Comput. Phys. Commun.* 182 (2011) **490**, [arXiv:1005.1481].

[10] R.D. Ball *et al.* [NNPDF Collaboration], *JHEP* 1504 (2015) 040, [arXiv:1410.8849].

[11] B. Pötter, *Comput. Phys. Commun.* 133 (2000) 105, [hep-ph/9911221].

[12] T. Biekötter, M. Klasen and G. Kramer, *Phys. Rev.* **D92** (2015) 7, 074037, [arXiv:1508.07153].

[13] V. Bertone, S. Carrazza and J. Rojo, *Comp. Phys. Comm.* 185 (2014) 1647, [arXiv:1310.1394].
     V. Bertone, private communication, July 2016.

[14] S. Forte, E. Laenen, P. Nason and J. Rojo, *Nucl. Phys.* **B834** (2010) 116, [arXiv:1001.2312].

[15] J. Currie, T. Gehrmann and J. Niehues, *Phys. Rev. Lett.* 117 (2016) 042001, [arXiv:1606.03991].

[16] A. Gehrmann-De Ridder, T. Gehrmann, E.W.N. Glover, A. Huss and T.A. Morgan, *JHEP* 1607 (2016) 133, [arXiv:1605.04295].

[17] H. Spiesberger, *Conf. Proc.* C98-04-27 (1998) 530, EPRC91.

[18] HERAFitter Collaboration, S. Alekhin *et al.*, *Eur.Phys.J.* **C75** (2015) 304, [arXiv:1410.4412].

[19] ZEUS Collaboration, H. Abramowiczet *et al.*, *Nucl. Phys.* **B864** (2012) 1, [arXiv:1205.6153].

[20] G. Dissertori, A. Gehrmann-De Ridder, T. Gehrmann, E. W. N. Glover, G. Heinrich and H. Stenzel, JHEP 0802 (2008) 040, [arXiv:0712.0327].

[21] JADE Collaboration, J. Schieck *et al.*, *Eur. Phys. J.* **C48** (2006) 3 [Erratum-ibid. C50(2007) 769], [arXiv:0707.0392].

[22] OPAL Collaboration, G. Abbiendi *et al.*, *Eur. Phys. J.* **C71** (2011) 1733, [arXiv:1101.1470].

[23] CMS Collaboration, V Khachatryan *et al.*, *Eur.Phys.J.* **C75** (2015) 186, [arXiv:1412.1633].

[24] D0 Collaboration, V. Abazov *et al.*, *Phys. Lett.* **B718** (2012) 56, [arXiv:1207.4957]

[25] PDF Collaboration, K. A. Olive *et al.*, *Chin. Phys.* **C38** (2014) 090001 (2015 update); and S. Bethke, G. Dissertori, G. Salam.
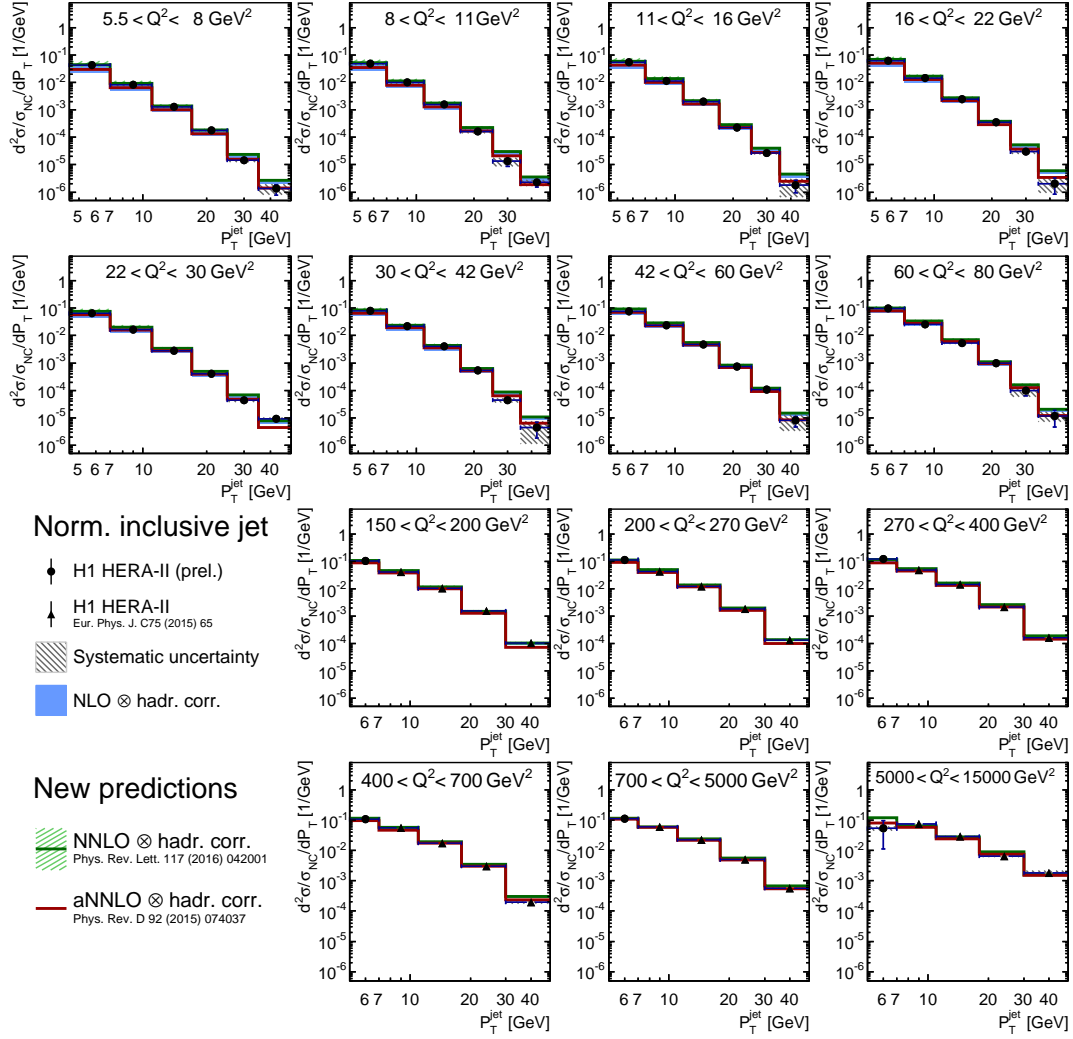
Figure 1: Double-differential cross sections for normalised inclusive jet production in neutral-current DIS as function of Q^2 and P_T^{jet}. The vertical error bars indicate the statistical uncertainties. The shaded areas around the data points show the systematic uncertainties from the variation of the jet energy scale, cluster energy scale, electron angle and electron energy as well as the model uncertainty. The data are compared to NLO predictions, approximate NNLO and full NNLO predictions. The bands on the theory predictions indicate the uncertainties from the so-called 'asymmetric 6-point' scale variation. The triangles show the measurement from ref. [3]. The statistical correlation with the dijet and trijet measurements are shown in figure 7. The data are divided by the P_T^{jet} bin size for better visibility.
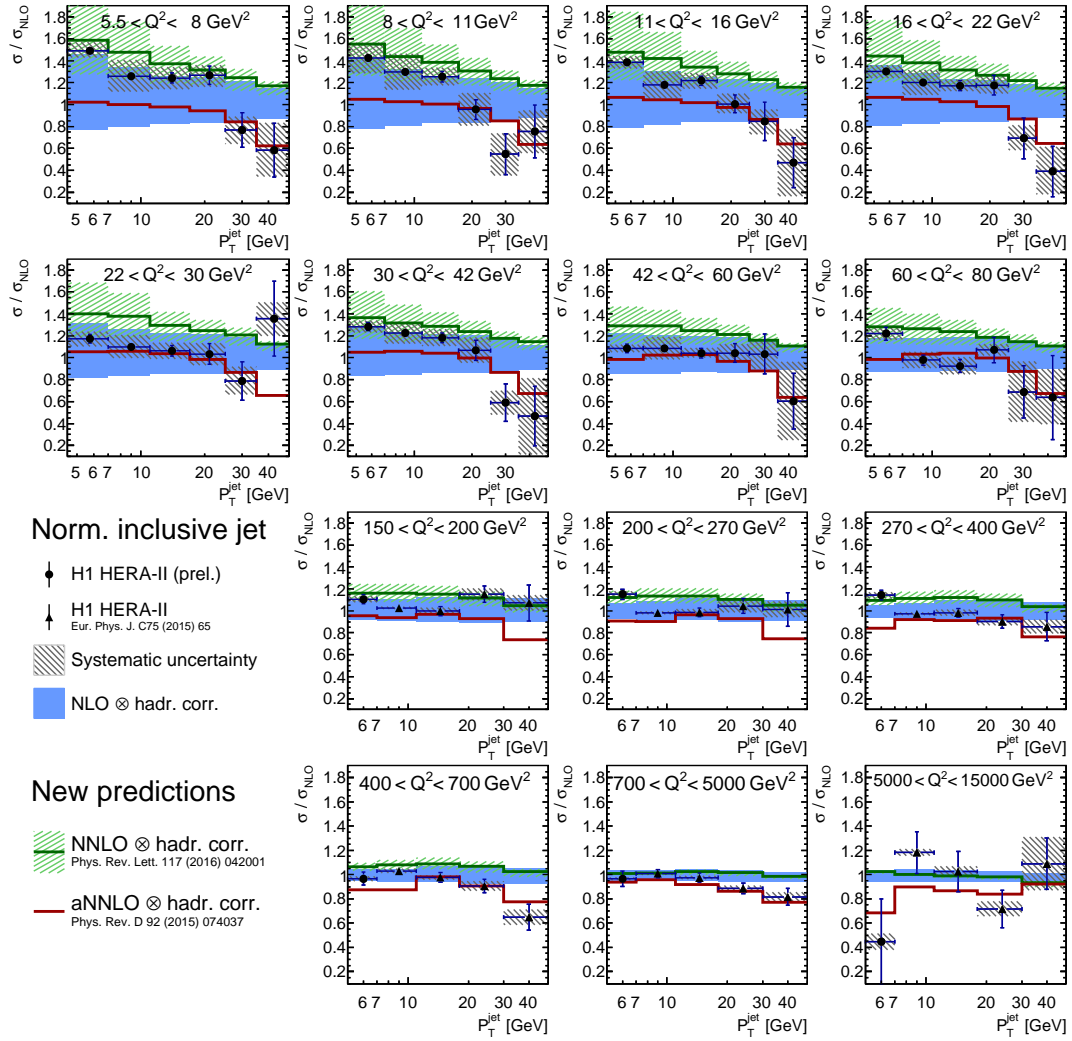
Figure 2: Ratio of normalised inclusive jet cross sections, NNLO and aNNLO predictions to the NLO predictions. Other details as in fig. 1.
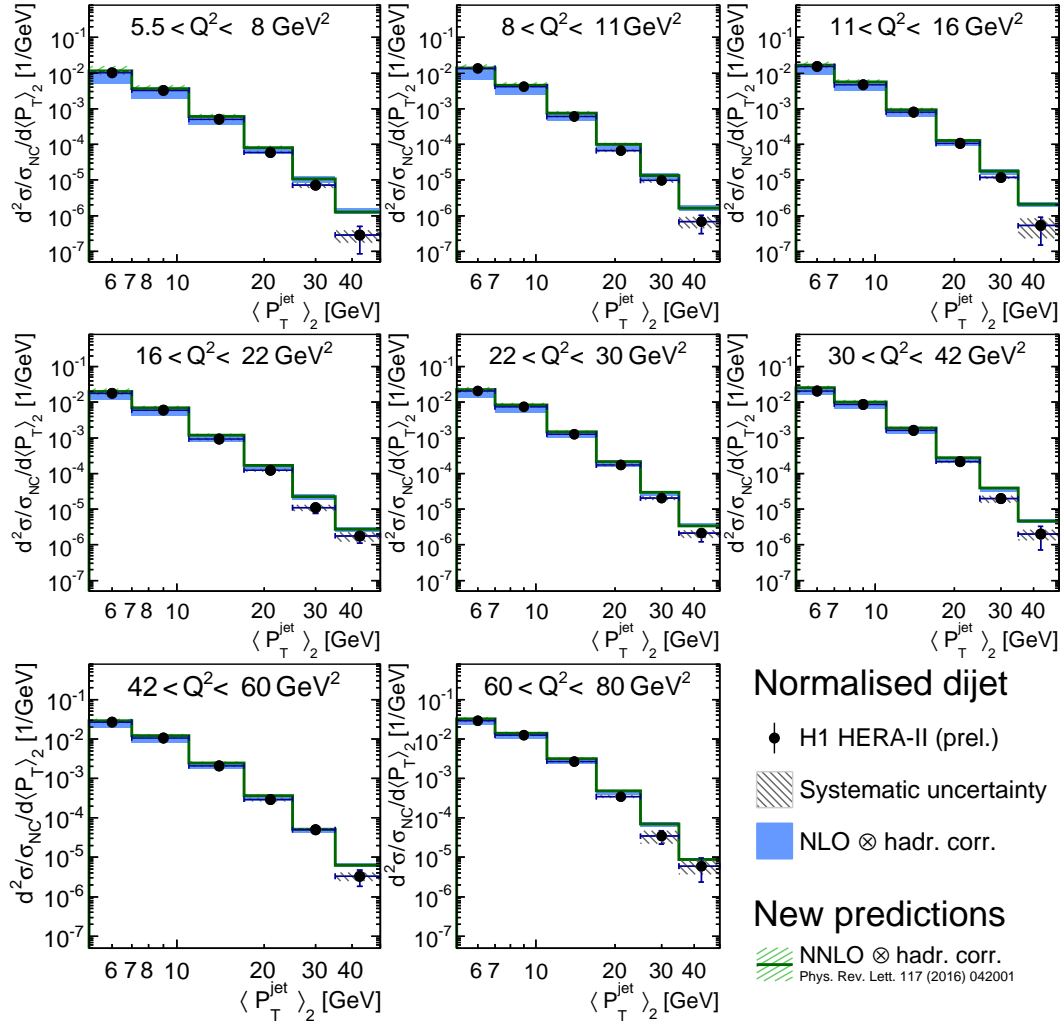
Figure 3: Double-differential cross sections for normalised dijet production in NC DIS as a function of Q^2 and $\langle P_T \rangle_2$. Other details as in fig. 1.

9
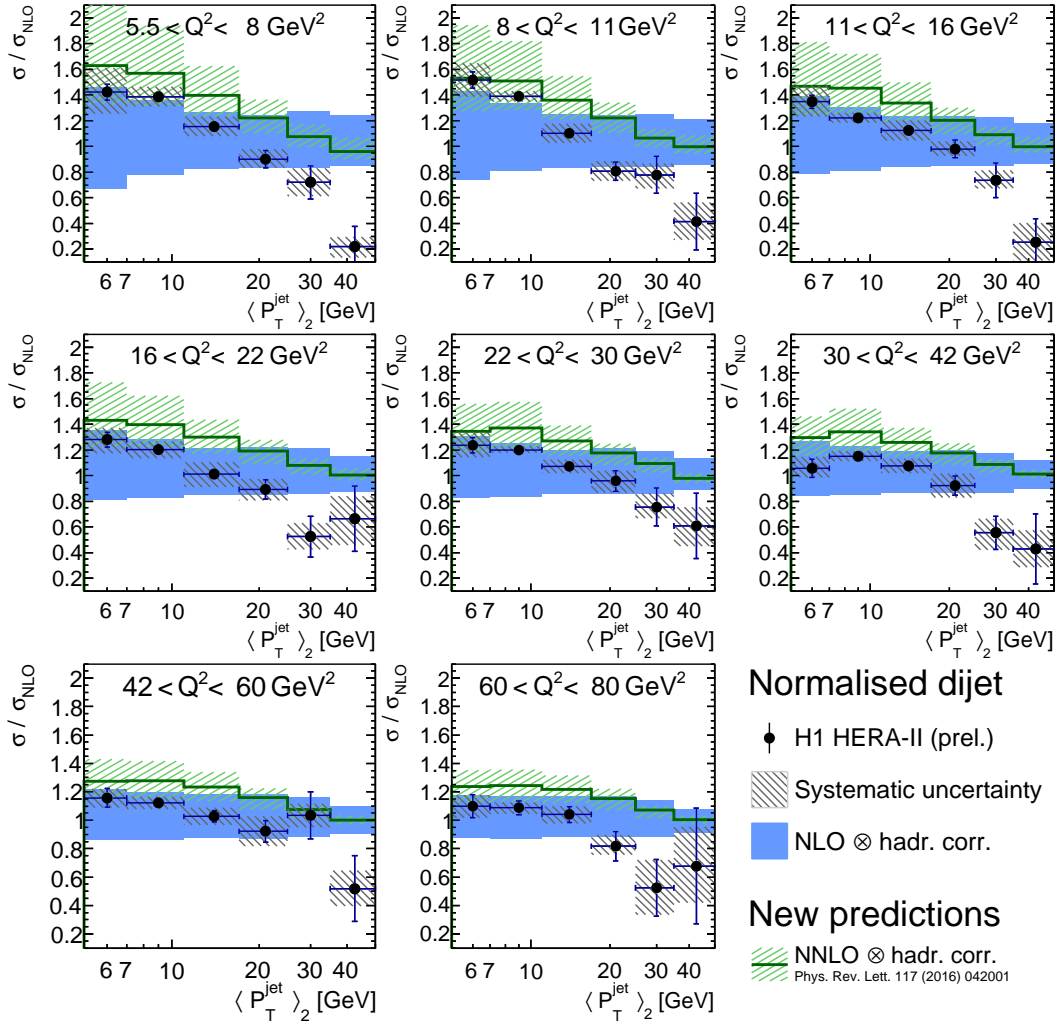
Figure 4: Ratio of normalised dijet cross sections and NNLO predictions to NLO predictions. Other details as in fig. 1.
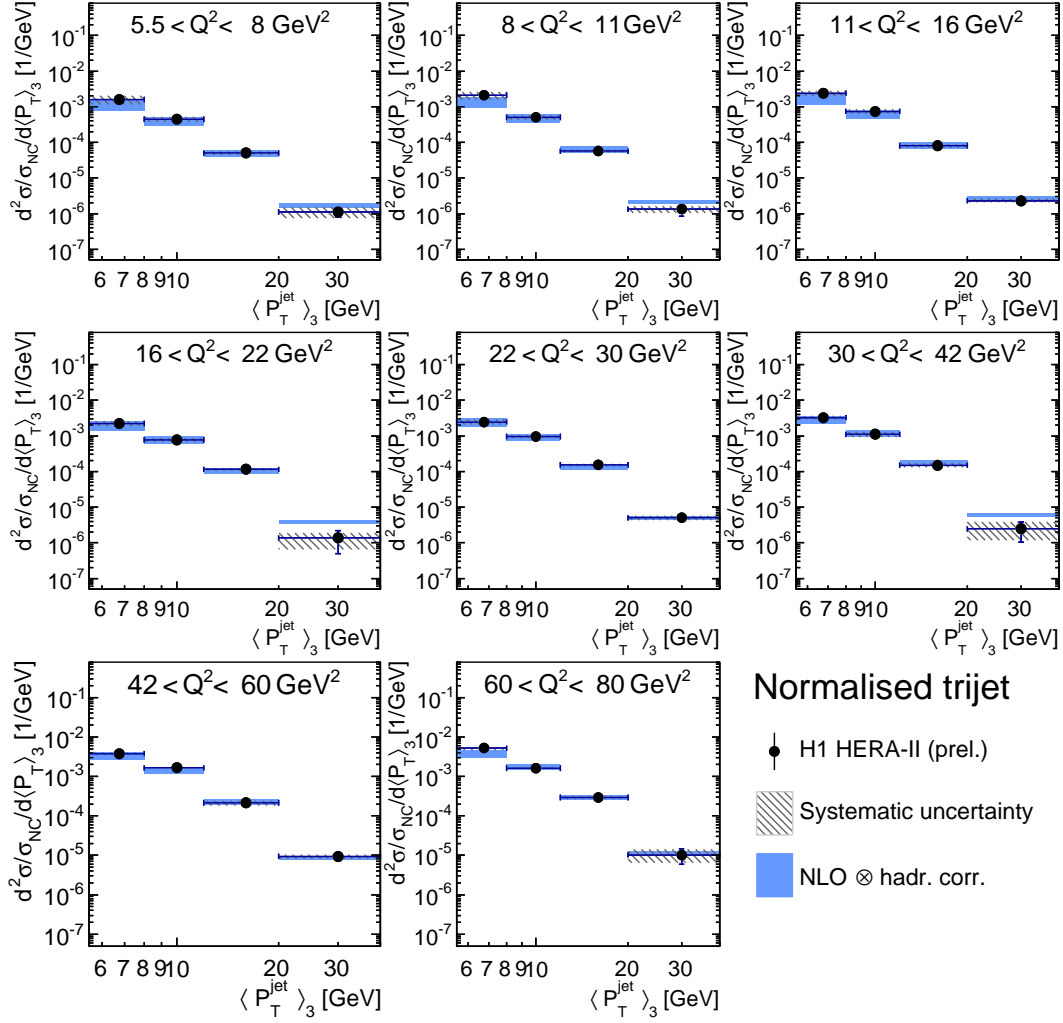
Figure 5: Double-differential cross sections for normalised trijet production in NC DIS as a function of Q^2 and $\langle P_T \rangle_3$. Other details as in fig. 1.
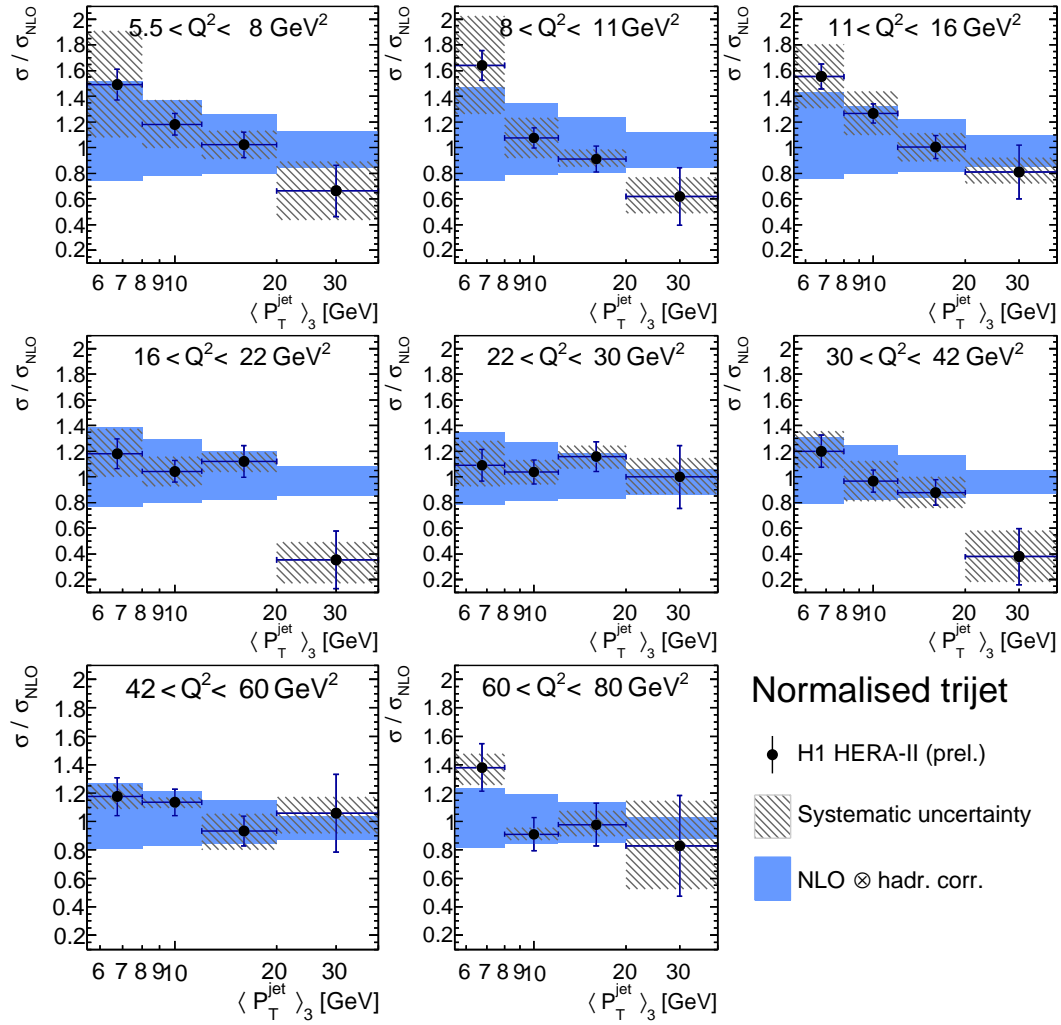
Figure 6: Ratio of normalised trijet cross sections to NLO predictions. Other details as in fig. 1.
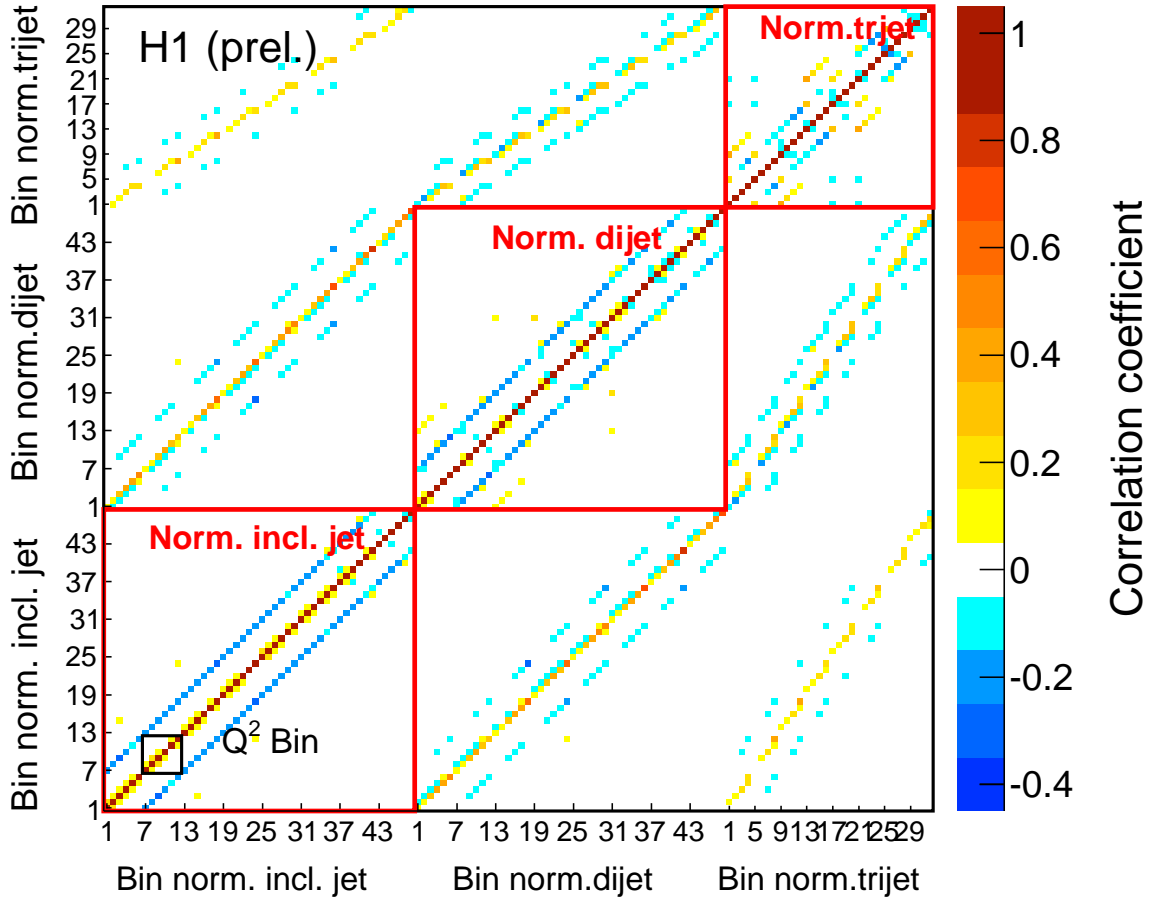
Figure 7: Correlation coefficients of the statistical uncertainty of the three unfolded normalised cross section measurements. The axis labels denote the bin numbers of the respective jet measurement. As example, the black box indicates the four $P_\mathrm{T}^\mathrm{jet}$ bins in one Q^2 bin of the inclusive jet data. The correlations between the measurements are known since they are measured on detector-level and propagated through the unfolding procedure. The calculation of the normalised jet cross sections takes the statistical correlation of the absolute jet cross sections and the NC DIS cross sections into account.
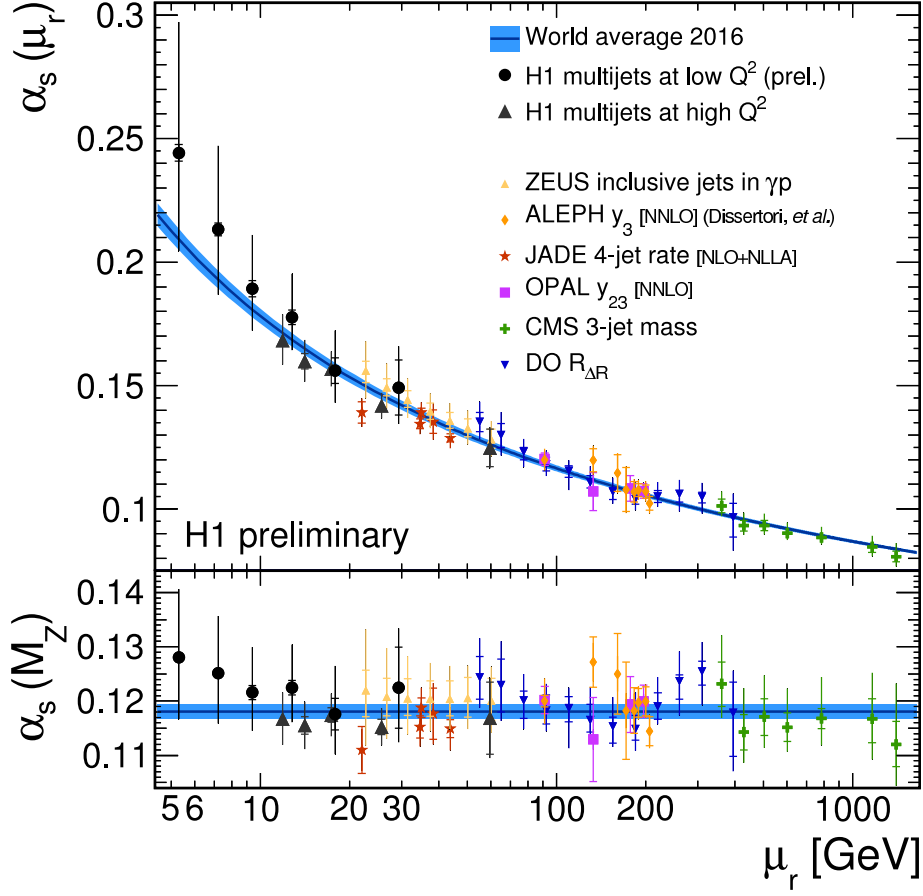
Figure 8: Values of $\alpha_s(M_Z)$ extracted from the normalised inclusive jet, dijet and trijet cross sections using NLO predictions compared to values extracted from other jet data. The upper panel shows the values of the strong coupling $\alpha_s(\mu_r)$ and the lower panel the equivalent values of $\alpha_s(M_Z)$ for all measurements. The full circles show the extracted values from the low-Q^2 normalised inclusive jet, dijet and trijet data as outlined in the text. The inner error bars indicate the experimental uncertainty, while the full error bars indicate the total uncertainty, including the experimental and theoretical contributions. The solid line shows the world average value of $\alpha_s(M_Z) = 0.1181 \pm 0.0013$ [25], and its value evolved to μ_r using the solution of the QCD renormalisation group equation. Also shown are the values of α_s from multijet measurement at high values of Q^2 by H1 [3] (dark triangles), from inclusive jet measurements in photoproduction by the ZEUS experiment [19] (upper triangles), from the 3-jet rate y_3 in a fit of NNLO calculations [20] to ALEPH data taken at LEP (diamonds), from the 4-jet rate measured by the JADE experiment at PETRA [21] (stars), from the jet transition value y_{23} measured by OPAL at LEP [22] (squares), from 3-jet mass cross sections as measured by the CMS experiment at the LHC [23] (crosses). and from jet angular correlations $R_{\Delta R}$ by the D0 experiment at the Tevatron (lower triangles) [24]

14